

**High pressure electrochemical reduction of CO<sub>2</sub> to formic acid/formate  
A comparison between bipolar membranes and cation exchange membranes**

Ramdin, Mahinder; Morrison, Andrew R.T.; de Groen, Mariette; van Haperen, Rien; De Kler, Robert; Van Den Broeke, Leo J.P.; Trusler, J. P.Martin; De Jong, Wiebren; Vlugt, Thijs J.H.

**DOI**

[10.1021/acs.iecr.8b04944](https://doi.org/10.1021/acs.iecr.8b04944)

**Publication date**

2019

**Document Version**

Final published version

**Published in**

Industrial and Engineering Chemistry Research

**Citation (APA)**

Ramdin, M., Morrison, A. R. T., de Groen, M., van Haperen, R., De Kler, R., Van Den Broeke, L. J. P., Trusler, J. P. M., De Jong, W., & Vlugt, T. J. H. (2019). High pressure electrochemical reduction of CO<sub>2</sub> to formic acid/formate: A comparison between bipolar membranes and cation exchange membranes. *Industrial and Engineering Chemistry Research*, 58(5), 1834–1847. <https://doi.org/10.1021/acs.iecr.8b04944>

**Important note**

To cite this publication, please use the final published version (if applicable).  
Please check the document version above.

**Copyright**

Other than for strictly personal use, it is not permitted to download, forward or distribute the text or part of it, without the consent of the author(s) and/or copyright holder(s), unless the work is under an open content license such as Creative Commons.

**Takedown policy**

Please contact us and provide details if you believe this document breaches copyrights.  
We will remove access to the work immediately and investigate your claim.

# High Pressure Electrochemical Reduction of CO<sub>2</sub> to Formic Acid/Formate: A Comparison between Bipolar Membranes and Cation Exchange Membranes

Mahinder Ramdin,<sup>†</sup> Andrew R. T. Morrison,<sup>‡</sup> Mariette de Groen,<sup>§</sup> Rien van Haperen,<sup>§</sup> Robert de Kler,<sup>§</sup> Leo J. P. van den Broeke,<sup>§</sup> J. P. Martin Trusler,<sup>||</sup> Wiebren de Jong,<sup>‡</sup> and Thijs J. H. Vlught<sup>\*,†</sup>

<sup>†</sup>Engineering Thermodynamics, Process & Energy Department, Faculty of Mechanical, Maritime and Materials Engineering, Delft University of Technology, Leeghwaterstraat 39, 2628CB Delft, The Netherlands

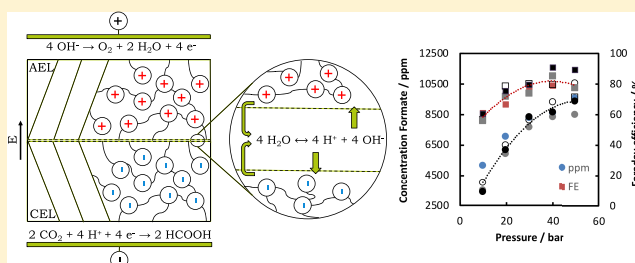
<sup>‡</sup>Large-Scale Energy Storage, Process & Energy Department, Faculty of Mechanical, Maritime and Materials Engineering, Delft University of Technology, Leeghwaterstraat 39, 2628CB Delft, The Netherlands

<sup>§</sup>Coval Energy, Wilhelminasingel 14, 4818AA Breda, The Netherlands

<sup>||</sup>Imperial College London, South Kensington Campus, London SW7 2AZ, United Kingdom

## Supporting Information

**ABSTRACT:** A high pressure semicontinuous batch electrolyzer is used to convert CO<sub>2</sub> to formic acid/formate on a tin-based cathode using bipolar membranes (BPMs) and cation exchange membranes (CEMs). The effects of CO<sub>2</sub> pressure up to 50 bar, electrolyte concentration, flow rate, cell potential, and the two types of membranes on the current density (CD) and Faraday efficiency (FE) for formic acid/formate are investigated. Increasing the CO<sub>2</sub> pressure yields a high FE up to 90% at a cell potential of 3.5 V and a CD of ~30 mA/cm<sup>2</sup>. The FE decreases significantly at higher cell potentials and current densities, and lower pressures. Up to 2 wt % formate was produced at a cell potential of 4 V, a CD of ~100 mA/cm<sup>2</sup>, and a FE of 65%. The advantages and disadvantages of using BPMs and CEMs in electrochemical cells for CO<sub>2</sub> conversion to formic acid/formate are discussed.



## INTRODUCTION

The concept of producing chemicals and fuels from electricity, instead of fossil fuels, utilizing the intermittent behavior of renewable energy sources (i.e., power-to-X (P2X) concepts), has recently gained considerable interest from researchers aiming at reducing CO<sub>2</sub> emissions.<sup>1–7</sup> For example, CO<sub>2</sub> can be converted in an electrochemical cell to various value-added products such as acids, alcohols, hydrocarbons, and syngas.<sup>8–13</sup> The selectivity of the different products depends on many process variables such as the type of catalyst and its morphology, temperature, pressure, potential and current density, pH, electrolyte type and concentration, aqueous or nonaqueous solvent, flow characteristics, impurities, membranes, cell design, etc.<sup>14–22</sup> In aqueous solvents or solvents containing substantial amounts of water, the hydrogen evolution reaction (HER) is always in competition with the CO<sub>2</sub> reduction reaction (CRR).<sup>23–25</sup> This is because the solubility of CO<sub>2</sub> in water at standard conditions is low, which causes significant mass transfer limitations. To overcome this limitation, the use of nonaqueous solvents, gas-diffusion electrodes (GDEs), high CO<sub>2</sub> pressures, and cathodes which possess high overpotentials for the HER have been

proposed.<sup>14,26–31</sup> However, the selectivity of an electrode for a certain product can change dramatically depending on the choice of the solvent. For example, the main product of CO<sub>2</sub> electrolysis on tin (Sn) or lead (Pb) electrodes in aqueous media is formic acid or formate, but this changes to oxalic acid/oxalate when a nonaqueous solvent is used.<sup>32,33</sup> Although GDEs have the potential to achieve high current densities, complex manufacturing techniques are required to assemble the different porous layers for optimal performance.<sup>34–37</sup> Despite all efforts in past years, it is still a challenge to find a stable catalyst and process conditions, which allow obtaining simultaneously a high Faraday efficiency (FE) and current density (CD) for a sufficiently long time. In practice this would mean that one has to compromise between capital expenditure (CAPEX), which is dictated by the CD, and operating expenditure (OPEX), which is mainly governed by the FE.<sup>38–42</sup> For a fixed product output, a low CD will require

Received: October 9, 2018

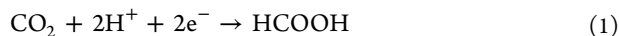
Revised: January 7, 2019

Accepted: January 14, 2019

Published: January 14, 2019

larger electrode surface areas, which will increase the size of the electrolyzer. A low FE will demand an increased input of resources (e.g., electricity, reactants) and additional downstream separation/recycling steps.

In this work, a high pressure semicontinuous batch electrolyzer is used to convert CO<sub>2</sub> to formic acid (HCOOH)/formate (HCOO<sup>-</sup>), which is one of the simplest chemicals, requiring only 2 mol of electrons per mole of product, that can be obtained in an aqueous solvent. Formic acid (FA) is an interesting molecule, because it can be decomposed to hydrogen (decarboxylation) or carbon monoxide (decarbonylation).<sup>43–46</sup> FA is produced from CO<sub>2</sub> according to the following electrochemical half-cell reaction:



The standard reduction potential of this reaction is  $-0.199$  V vs NHE at 298.15 K.<sup>19</sup> Note that this reaction does not imply a molecular mechanism, but it merely shows that two protons and electrons are required to obtain FA. Formic acid is a weak carboxylic acid with a pK<sub>a</sub> value of 3.74, which means that FA is only present in undissociated form at very low pH values.<sup>47</sup> Therefore, CO<sub>2</sub> electroreduction at low pressures in alkaline solutions will mainly yield formate (i.e., the conjugate base of FA). However, as can be observed in Figure S1 of the Supporting Information, the pH of bicarbonate solutions drops significantly when high pressure CO<sub>2</sub> is dissolved. For this reason, whenever we refer to formic acid or formate in this paper, we essentially mean a mixture of both, whose distribution is governed by the pH. A tin-based electrode is used as the cathode, since it is known to exhibit a high Faraday efficiency (FE) toward formic acid production. Typically, an ion exchange membrane is used to prevent oxidation of the (liquid) products formed at the cathode, to avoid mixing of gaseous anodic (e.g., O<sub>2</sub>) and cathodic (e.g., H<sub>2</sub>) products, and to allow the use of different anolytes and catholytes (i.e., different pH conditions). Here, we investigate the effect of bipolar membranes (BPMs) and cation exchange membranes (CEMs) on the performance of the electrochemical reduction of CO<sub>2</sub>. Anion exchange membranes (AEMs) were not tested in this study, because they exhibit a high formate crossover rate.<sup>48</sup> A CEM is a monopolar membrane with fixed negative charges, which allows cations to pass, but rejects anions.<sup>49</sup> A bipolar membrane is obtained by lamination of a positively charged anion exchange layer (AEL) and a negatively charged cation exchange layer (CEL), which are selective for anions and cations, respectively.<sup>50,51</sup> BPMs can be operated in two modes: (a) forward bias ( $V > 0$ ), where the CEL of the membrane faces the anode, and (b) reverse bias ( $V < 0$ ), where the CEL faces the cathode. In the forward bias mode, the electric field causes the mobile ions to migrate toward the interfacial region (IR), resulting in an accumulation of ions at the junction, which compensates the charges in the layers, thus decreasing the selectivity of the membrane.<sup>52,53</sup> As shown in Figure 1, in the reverse bias mode, applying a sufficiently high potential over the membrane will result in water splitting at the AEL–CEL interface due to (1) chemical reactions of water with functional groups in the membrane, and (2) an enhanced electric field effect, which can be described by Onsager's theory of the second Wien effect.<sup>50,54–60</sup> The H<sup>+</sup> and OH<sup>-</sup> ions will migrate through the CEL and AEL, respectively. In the reactor, the protons are then used in the CRR or HER, while the hydroxide ions are discharged at the anode to produce water, oxygen, and electrons.

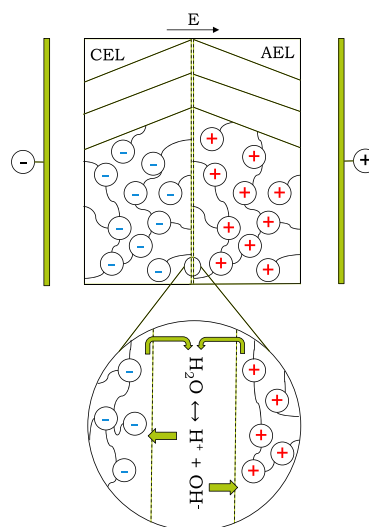


**Figure 1.** Operating principle of a BPM in reverse bias mode. Applying a sufficiently high potential over the membrane will result in enhanced water dissociation at the AEL–CEL interface, where the protons and hydroxide ions migrate through the CEL and AEL, respectively. The black arrow indicates the direction of the electric field.

Bipolar membranes have several additional benefits over monopolar ion exchange membranes, such as (1) BPMs allow the use of two different electrolyte solutions while maintaining a constant pH gradient over the membrane, (2) the product crossover is lower, and (3) acidification and basification can be performed without addition of acids and bases.<sup>49,51,61</sup> So far, BPMs have been applied in the electro dialysis process for acid and base production, CO<sub>2</sub> separation, water electrolysis, photoelectrolysis, fuel cells, water desalination, and, recently, CO<sub>2</sub> electrolysis.<sup>48,49,62–75</sup> To the best of our knowledge, BPMs have not been used previously for high pressure CO<sub>2</sub> electrolysis to formic acid/formate.

In this work, for the first time, CO<sub>2</sub> electrolysis to formic acid/formate is performed at high pressures (up to 50 bar) using bipolar membranes. The experiments were also executed with cation exchange membranes to benchmark the performance of the BPMs. In addition, the effects of electrolyte flow rate, electrolyte concentration, CO<sub>2</sub> pressure, and cell potential on the Faraday efficiency of formate and current density are investigated. The advantages and disadvantages of using BPMs and CEMs for CO<sub>2</sub> electrolysis are discussed.

## ■ EXPERIMENTAL SECTION

An overview of the high pressure experimental setup is shown in Figure 2. The core of the setup is a high pressure electrochemical reactor, which can be operated up to 80 bar. In Figure 3, an exploded view of the reactor is shown. The cell is divided into two compartments using either a bipolar ( $\sim 160$   $\mu\text{m}$ , Fumasep FBM-PK, Fumatech) or a cation exchange ( $\sim 130$   $\mu\text{m}$ , Fumasep FKB-PK, Fumatech) membrane. The cathodic compartment ( $\sim 100$  mL) is pressurized with high pressure CO<sub>2</sub> (99.999%, Linde Gas) from a gas cylinder, and the catholyte is recirculated continuously with an HPLC pump (Varian ProStar 210). The anodic compartment ( $\sim 200$  mL) can be pressurized by either a CO<sub>2</sub> or a N<sub>2</sub> gas cylinder, where the latter is used when supercritical CO<sub>2</sub> is required in the cathode compartment. In this case, the CO<sub>2</sub> in the cathodic compartment is pressurized through the accumulator. The

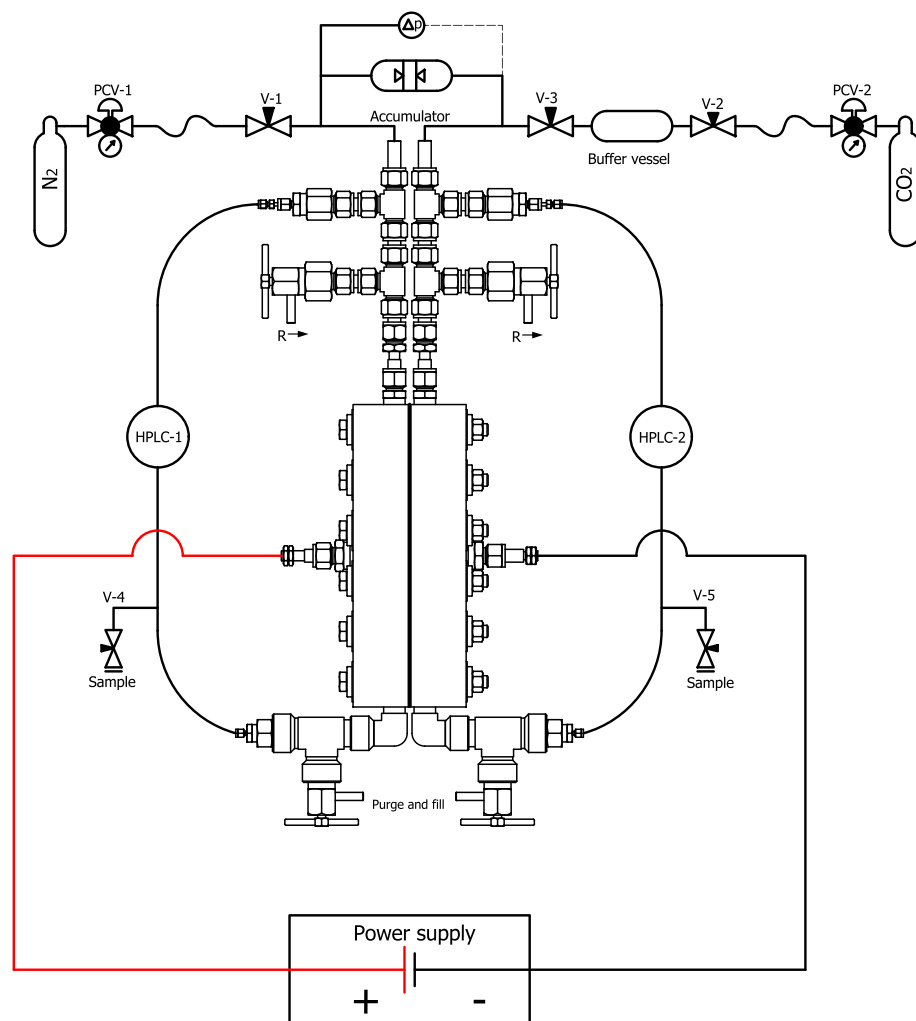


**Figure 2.** Overview of the high pressure experimental setup. At the core is a high pressure electrochemical reactor, which is divided into two compartments using an ion exchange membrane. The anolyte and catholyte were pressurized by  $N_2$  and/or  $CO_2$  gas cylinders and recirculated with HPLC pumps. An accumulator was used to eliminate pressure differences between both compartments and to prevent mixing of gaseous reactants and products. The electrochemical experiments were performed at fixed cell potentials using a lab power supply.

anodic and cathodic environment is separated by an accumulator, which prevents mixing of gases from both compartments and eliminates pressure differences over the membrane. The pressure difference over the membrane and the absolute pressure are measured with a differential pressure meter (Kobold, MAN-BF26-B4-A4-K) and a manometer ( $\pm 1$  bar, Swagelok), respectively. A tin-based electrode (99.99%, ElectroCell) with a surface area of  $\sim 140$   $cm^2$  and an iridium mixed metal oxide (Ir-MMO, Magneto Special Anodes) mesh ( $\sim 180$   $cm^2$ ) were used as the cathode and anode, respectively. We note, however, that the spacer covered a part of the cathode, which leads to a reactive surface area of the cathode of  $\sim 80$   $cm^2$ . The volume of the anodic compartment and the surface area of the anode were larger than the volume of the cathodic compartment and the surface area of the cathode. The reason for this is that the anodic processes (e.g., oxygen evolution and water transport to the BPM) should not be the limiting factor for the cathodic  $CO_2$  reduction reaction. The gap between the electrodes and the membrane was approximately 1 mm, which means that the electrode-to-electrode distance was  $\sim 2$  mm. The electrolytes potassium hydroxide (98% KOH), potassium bicarbonate (99.5%

$KHCO_3$ ), and sulfuric acid (95%  $H_2SO_4$ ) were purchased from Sigma-Aldrich and were used as received.

In a typical experiment, the reactor was loaded with approximately 200 mL of an anolyte and 100 mL of a catholyte, which was pressurized with high pressure  $CO_2$  and recirculated for 1 h with an HPLC pump ( $\sim 10$  mL/min) until saturation. Subsequently, electrolysis of  $CO_2$  was performed for 20 min at a fixed cell potential using a lab power supply (Votcraft DPPS-16-40). All experiments were performed at room temperature ( $22 \pm 1$   $^\circ C$ ). During the experiments, the  $CO_2$  in the buffer vessel was regularly flushed to prevent accumulation of gaseous reaction products, which might otherwise change the partial pressure of  $CO_2$ . At the end of each experiment, the anodic and cathodic compartments were completely emptied and the catholyte was analyzed for formic acid. The anolyte was only sampled randomly to determine the crossover of formic acid through the membranes. An ion chromatograph (Dionex DX-120, 4 mm AG14/AS14 guard and analytical column) with suppressed conductivity detection was used to measure the formate concentration in the anolyte and catholyte. The flow rate of the eluent (1 mM  $Na_2CO_3$ /1 mM  $NaHCO_3$  solution) was 1 mL/min. A pure standard of

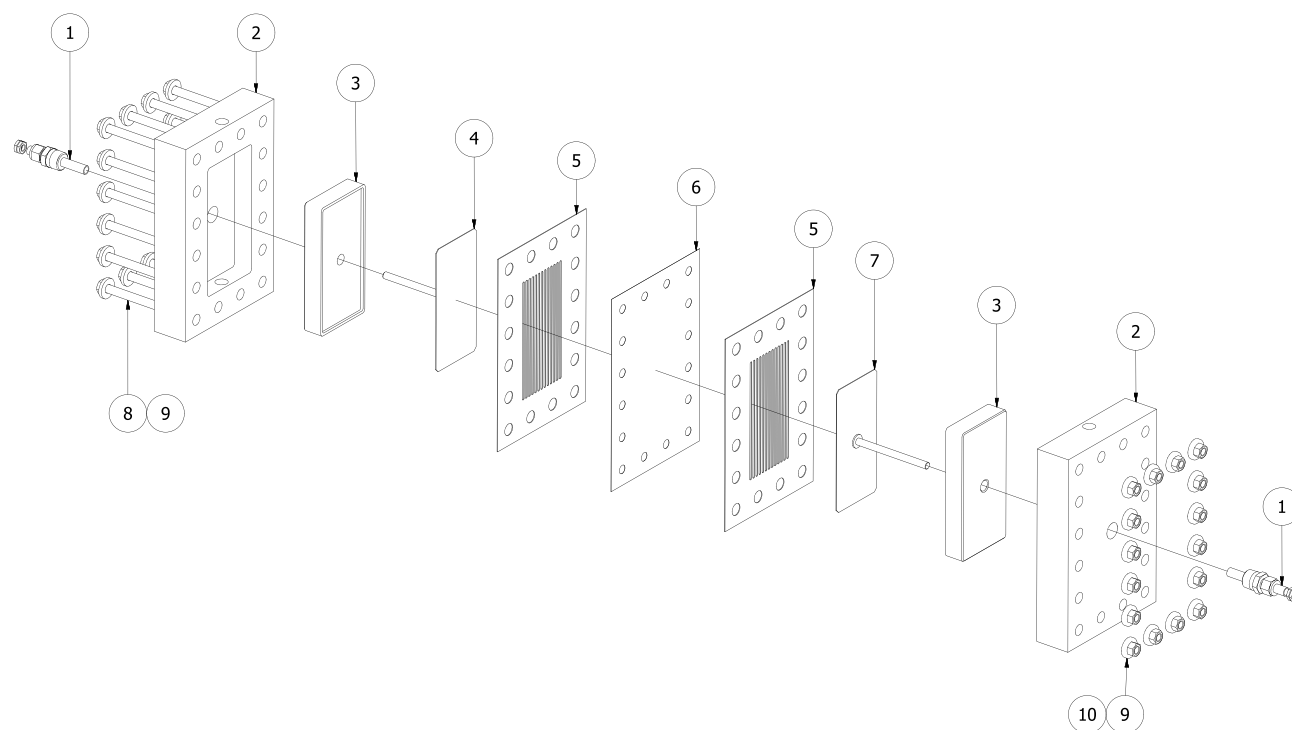


**Figure 3.** Exploded view of the reactor. (1) Insulator, (2) reactor shell, (3) Teflon fluid distributor, (4) anode, (5) Teflon spacer and seal, (6) membrane, (7) cathode, (8) hex head bolt, (9) isolating washer, and (10) hex nut.

formic acid (Sigma-Aldrich) was used to calibrate the equipment for quantitative analysis.

It is well-known that tin-based electrodes can be affected by degradation/deactivation under cathodic polarization.<sup>76</sup> Therefore, after each experiment, the cathode was chemically treated with a 5% nitric acid (HNO<sub>3</sub>) solution to remove possible deposits from the surface. Using a CEM with concentrated (>0.5M) H<sub>2</sub>SO<sub>4</sub> solutions as the anolyte resulted in some yellow sulfur-like deposition on the Ir-MMO anode surface, which was removed by reaction with a concentrated KOH solution. After treating the electrodes, both compartments were thoroughly rinsed with demineralized water and refilled with fresh electrolytes for the next experiment. The (bipolar) membranes were susceptible to abrupt pressure changes and startup/shutdown of the power supply. Therefore, the membranes were replaced after 15 pressurizing/depressurizing cycles. The reproducibility of the data was verified by repeating the experiments at least twice at the same operating conditions, but using fresh electrodes.

The Faraday efficiency and the current density are two important performance indicators in electrochemistry, just as selectivity and reaction rate are in traditional chemistry. The FE is a measure of how selectively electrons are transferred in an electrochemical reaction to the desired product. The FE (%) for formic acid/formate is calculated from

$$FE = \frac{FnVC^{\text{exp}}}{ItM_w} \times 100\% \quad (2)$$

where  $I$  is the current (A = C/s),  $t$  is the total time of the experiments (s),  $M_w$  is the molecular weight of formic acid (g/mol),  $n$  is the number of electrons involved in the reaction (2 for formic acid),  $V$  is the volume of catholyte (m<sup>3</sup>),  $C^{\text{exp}}$  is the experimentally measured concentration of formic acid (g/m<sup>3</sup>), and  $F$  is the Faraday constant (C/mol). The uncertainty in the

FE can be evaluated from the individual uncertainties of the variables in eq 2 using the methods of error propagation:<sup>77</sup>

$$\frac{\delta FE}{FE} = \sqrt{\left(\frac{\delta V}{V}\right)^2 + \left(\frac{\delta C}{C}\right)^2 + \left(\frac{\delta I}{I}\right)^2 + \left(\frac{\delta t}{t}\right)^2} \quad (3)$$

Using the estimated uncertainties of  $V$  ( $\pm 1$  mL due to purging),  $C$  ( $\pm 1\%$  due to the accuracy of the ion chromatograph),  $I$  ( $\pm 0.05$  A due to the accuracy of reading), and  $t$  ( $\pm 20$  s due to manual startup/shutdown of the power supply), the expected uncertainty in FE is ca. 5%.

The CD is calculated as the ratio between the current and the reactive geometrical surface area of the cathode ( $\sim 80$  cm<sup>2</sup>). Since the current was not always constant during the experiments, the current versus time ( $I-t$ ) curve was integrated to obtain the total charge passage ( $Q$ ):

$$Q = \int_0^t I dt \quad (4)$$

The lab power supply allowed reading of the current to an accuracy of 0.05 A, which imparts an uncertainty of 60 C on  $Q$  for a total measurement time of 20 min or an uncertainty in the CD of  $\sim 0.6$  mA/cm<sup>2</sup>. The error due to the integration of eq 4 is within this uncertainty.

## RESULTS AND DISCUSSION

In the following, the effect of CO<sub>2</sub> pressure, electrolyte concentration, catholyte flow rate, and cell potential on the CRR will be discussed. In addition, we show that the interplay between electrodes, electrolytes, and membranes is crucial for an efficient design of CO<sub>2</sub> electrolyzers. Finally, the advantages and disadvantages of BPMs and CEMs for CO<sub>2</sub> electrolysis are discussed.

**Effect of CO<sub>2</sub> Pressure.** The aim of the first set of experiments was to investigate the effect of pressure on the electrochemical reduction of CO<sub>2</sub> to formate on a tin-based cathode using a BPM. In these experiments, the cell potential, temperature, pressures, flow rate, anolyte, and catholyte, were 3.5 V, 22 ± 1 °C, 5–50 bar, 10 mL/min, 1 M KOH, and 0.5 M KHCO<sub>3</sub>, respectively. The electrochemical experiments were performed as described in the [Experimental Section](#), and the results are shown in [Figure 4](#). Clearly, the concentration of

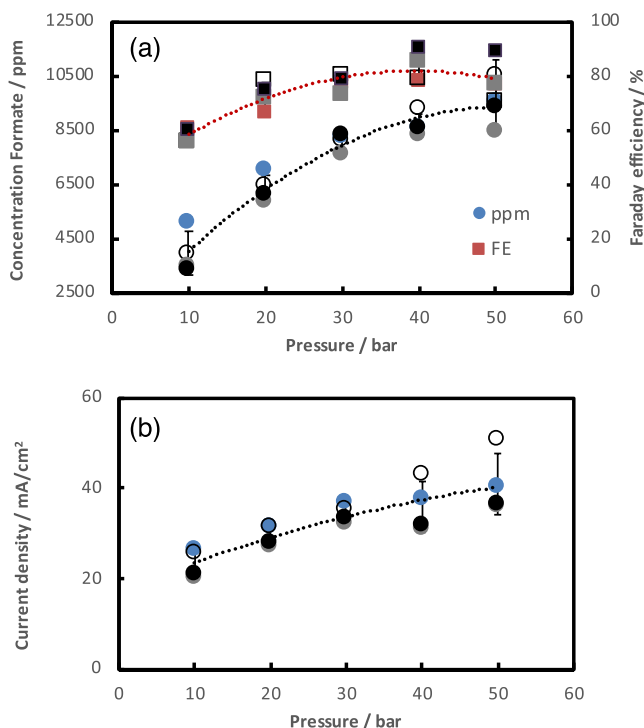


**Figure 4.** (a) Concentration of formate (circles) and Faraday efficiency (squares), and (b) current density as a function of pressure for CO<sub>2</sub> electrolysis at 3.5 V using a BPM. The anolyte, catholyte, flow rate, and electrolysis time were 1 M KOH, 0.5 M KHCO<sub>3</sub>, 10 mL/min, and 20 min. Data are shown for four different runs, where the dotted lines represent the arithmetic mean of the results.

formate, the FE, and the CD sharply increase as the CO<sub>2</sub> pressure is increased, but the FE seems to reach a plateau (~90%) around 40 bar. At these experimental conditions, increasing the pressure further does not improve the FE. In fact, a slight decrease in the FE is observed after a pressure of 40 bar, which is likely caused by (1) formate crossover through the BPM, and (2) a significant pH drop caused by high pressure CO<sub>2</sub> dissolution, which favors the HER. Analysis of the anolyte confirmed that approximately 1% formate passed through the BPM.

The effect of pressure on the performance of CO<sub>2</sub> electrolysis to formate using cation exchange membranes was also investigated. The first experiments with a CEM were performed at 3.5 V, 22 ± 1 °C, pressures between 10 and 50 bar, 0.5 M H<sub>2</sub>SO<sub>4</sub> as the anolyte, 1 M KHCO<sub>3</sub> as the catholyte, and a catholyte flow rate of 10 mL/min. In [Figure 5](#), the results of the three different runs are shown. The conclusions for the CEM are very similar to those for the BPM; the FE, CD, and the concentration of formate increase as the CO<sub>2</sub> pressure is increased. The FE shows a maximum of ~90% around a CO<sub>2</sub> pressure of 40 bar with a slight decrease thereafter, which is

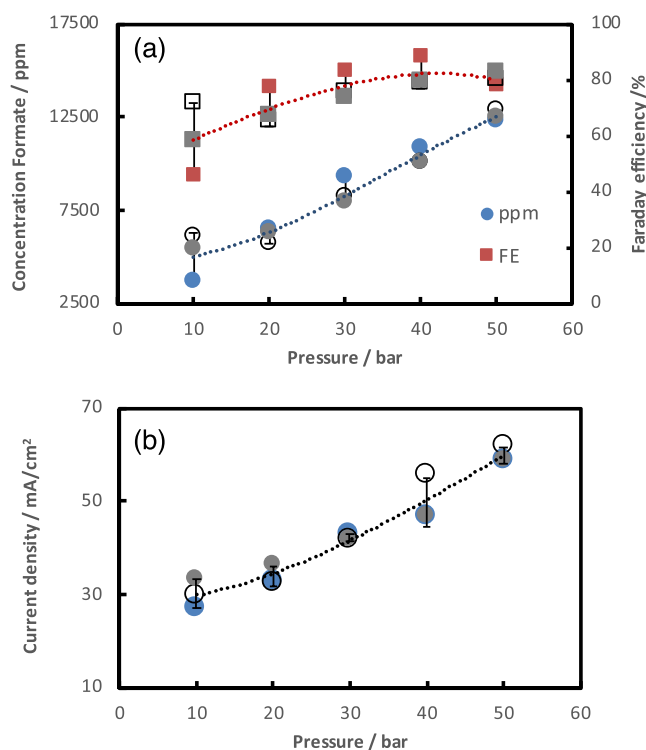
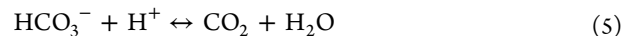


**Figure 5.** (a) Concentration of formate (circles) and Faraday efficiency (squares), and (b) current density as a function of pressure for CO<sub>2</sub> electrolysis at 3.5 V using a CEM. The anolyte, catholyte, flow rate, and electrolysis time were 0.5 M H<sub>2</sub>SO<sub>4</sub>, 1 M KHCO<sub>3</sub>, 10 mL/min, and 20 min. Data are shown for three different runs, where the dotted lines represent the arithmetic mean of the results.

again due to formate crossover through the CEM, and a pH drop caused by CO<sub>2</sub> dissolution. Analysis of the anolyte confirmed that around 5% of the formate passed through the CEM, which is known to have a substantially higher product crossover than BPMs. Otherwise, a comparison of [Figures 4](#) and [5](#) reveals that the performance of the CEM is very similar to that of the BPM. However, the CO<sub>2</sub> pressure seems to have a stronger influence on the FE of the CEM than for the BPM. A possible explanation for this is that as soon a potassium ion is pulled through the CEM, additional CO<sub>2</sub> becomes available via bicarbonate decomposition:



The equilibrium constant ( $K$ ) of this reaction equals

$$K = \frac{[\text{CO}_2]}{[\text{HCO}_3^-][\text{H}^+]} \quad (6)$$

Since the concentration of CO<sub>2</sub> in the solution is proportional to the pressure of CO<sub>2</sub>, the equilibrium is shifted toward the right as the pressure is increased. The consequence of this is that more CO<sub>2</sub> becomes available locally in the solution, which promotes the CRR and increases the FE for formate formation.

The overall behavior observed for the BPM and the CEM can be explained as follows. At low pressures, the CO<sub>2</sub> solubility is low and the protons coming from the BPM/CEM mainly participate in the HER, instead of the CRR, thereby decreasing the FE for formate. At high pressures, the low solubility problem is (partially) resolved, but now the low current density or proton availability starts to limit the electrochemical process. To maximize the selectivity, it is

important that  $\text{CO}_2$ , protons, and electrons are available in a correct stoichiometry at the electrode surface, which is qualitatively explained in Figure 6. Similar diagrams have

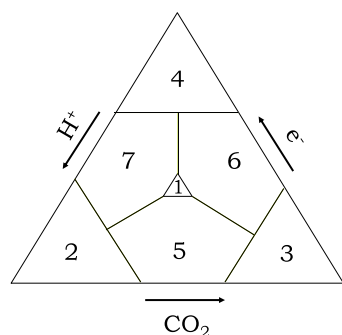


**Figure 6.** Qualitative triangular schematic diagram to explain the FE for  $\text{CO}_2$  electrolysis to formic acid/formate. Region 1 has a correct  $\text{CO}_2$ ,  $\text{H}^+$ , and  $e^-$  stoichiometry; region 2 is deficient in  $\text{CO}_2$  and electrons; region 3 is deficient in  $\text{H}^+$  and electrons; region 4 is deficient in  $\text{CO}_2$  and  $\text{H}^+$ ; region 5 is deficient in electrons; region 6 is deficient in  $\text{H}^+$ ; and region 7 is deficient in  $\text{CO}_2$ . The axes represent the concentrations of  $\text{CO}_2$ , electrons, and protons on a reaction site of the electrode.

been used by Hara et al.<sup>26</sup> and Li and Oloman<sup>78,79</sup> to explain product selectivities. Being a qualitative diagram, the size and boundaries of the regions in Figure 6 are chosen arbitrarily, but this will not interfere with the interpretation of the results. There is a small operating window, region 1 in Figure 6, where the supplies of  $\text{CO}_2$ , electrons, and protons are correctly balanced. In principle, it is possible to have a high FE at low CDs, but for formic acid the highest FE is observed at moderate CDs and not at the lowest CD.<sup>30</sup> For this reason, region 1 is not extended to the right corner (region 3) of Figure 6. In all the other regions in Figure 6, there is a deficiency in either  $\text{CO}_2$ , protons, or electrons, which will adversely affect the selectivity. For example, region 2 is deficient in  $\text{CO}_2$  and electrons, region 3 is deficient in  $\text{H}^+$  and electrons, region 4 is deficient in  $\text{CO}_2$  and  $\text{H}^+$ , region 5 is deficient in electrons, region 6 is deficient in  $\text{H}^+$ , and region 7 is deficient in  $\text{CO}_2$ . A deficiency in  $\text{CO}_2$ , electrons, and protons corresponds to a state which is limited by mass transfer, kinetics, and water splitting, respectively. The key is to find the operating conditions that satisfy the requirements for region 1, which is a challenging task since in electrochemistry many of these parameters (i.e., potential, current density, concentration, FE) are nonlinearly interrelated.

**Effect of Electrolyte Concentration.** The concentration of the catholyte can have a significant influence on the  $\text{CO}_2$  electrolysis performance. Therefore,  $\text{CO}_2$  electrolysis was performed at 3 V using a BPM, 1 M KOH as the anolyte, a flow rate of 10 mL/min, and catholytes with three different (0.1, 0.5, and 1 M)  $\text{KHCO}_3$  concentrations. As shown in Figure 7, the highest FE and CD are obtained when an intermediate concentration of 0.5 M  $\text{KHCO}_3$  is used. Using a high concentration of  $\text{KHCO}_3$  (1 M) has a detrimental effect on the electrochemical reduction of  $\text{CO}_2$ , which is consistent with the literature and can be explained as (1) the  $\text{CO}_2$  solubility decreases significantly due to a salting-out effect, (2) an increased adsorption of potassium ions on the electrode inhibits  $\text{CO}_2$  transport, (3) a buffering effect of  $\text{HCO}_3^-$  at the cathode, which decreases the surface pH as the bicarbonate

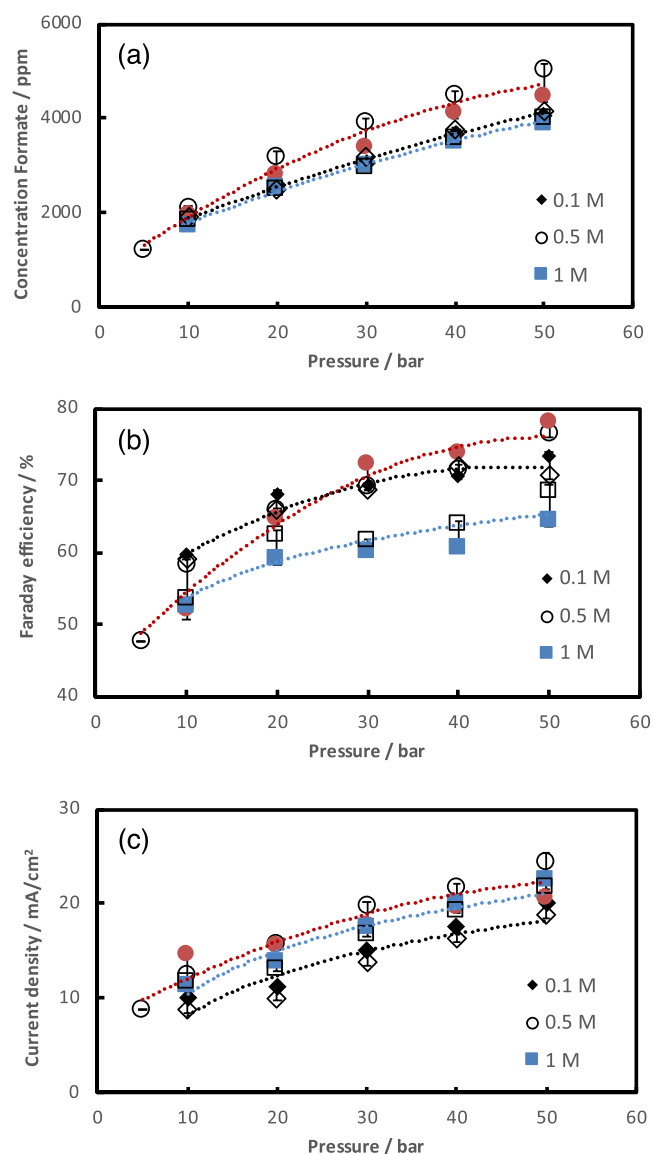


**Figure 7.** Effect of catholyte concentration on the (a) production of formate, (b) Faraday efficiency, and (c) current density as a function of pressure for  $\text{CO}_2$  electrolysis at 3 V using a BPM and 0.1 M  $\text{KHCO}_3$  (diamonds), 0.5 M  $\text{KHCO}_3$  (circles), and 1 M  $\text{KHCO}_3$  (squares) as the catholyte. The anolyte, flow rate, and electrolysis time were 1 M KOH, 10 mL/min, and 20 min. Results are shown for two different runs, where the dotted lines represent the arithmetic mean of the results.

concentration in the bulk is increased, and (4) the electric field is reduced, which destabilizes the CRR intermediates, thereby reducing the FE.<sup>78–82</sup> Using a low concentration of  $\text{KHCO}_3$  (0.1 M) suffers from a low conductivity and a significant pH drop due to high pressure  $\text{CO}_2$  dissolution. Both effects enhance the HER and reduce the FE for formate. Therefore, the performance of  $\text{CO}_2$  electrolysis in terms of the FE and CD is better for moderate  $\text{KHCO}_3$  concentrations: 0.5 M > 0.1 M > 1 M.

The effect of electrolyte concentration on the CRR using a CEM was also investigated.  $\text{CO}_2$  electrolysis was performed at 3.5 V, a flow rate of 10 mL/min, and three different combinations of anolyte ( $\text{H}_2\text{SO}_4$ ) and catholyte ( $\text{KHCO}_3$ ) concentrations, but keeping an anolyte to catholyte molar ratio of 1:2. The data in Figure 8 show that the combination of 0.5

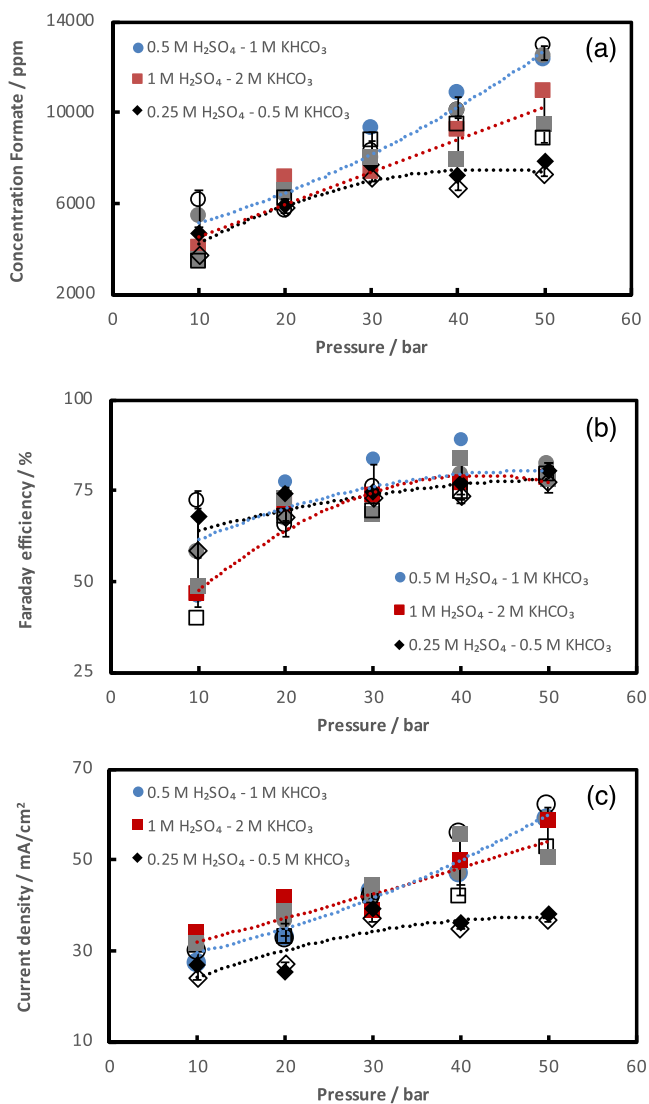


**Figure 8.** Effect of electrolyte concentration on the (a) formate production, (b) Faraday efficiency, and (c) current density as a function of pressure for CO<sub>2</sub> electrolysis at 3.5 V using a CEM. The anolyte, catholyte, flow rate, and electrolysis time were H<sub>2</sub>SO<sub>4</sub>, KHCO<sub>3</sub>, 10 mL/min, and 20 min. Three different concentrations of anolytes and catholytes were tested: 0.25 M H<sub>2</sub>SO<sub>4</sub>–0.5 M KHCO<sub>3</sub> (diamonds), 0.5 M H<sub>2</sub>SO<sub>4</sub>–1 M KHCO<sub>3</sub> (circles), and 1 M H<sub>2</sub>SO<sub>4</sub>–2 M KHCO<sub>3</sub> (squares). Results are shown for three different runs, where the dotted lines represent the arithmetic mean of the results.

M H<sub>2</sub>SO<sub>4</sub> and 1 M KHCO<sub>3</sub> gives the best results in terms of formate production, FE, and CD. The combination of 1 M H<sub>2</sub>SO<sub>4</sub> and 2 M KHCO<sub>3</sub> is slightly better than the combination of 0.25 M H<sub>2</sub>SO<sub>4</sub> and 0.5 M KHCO<sub>3</sub>, especially in the higher pressure range. The optimal catholyte concentration for the CEM seems to be around 1 M KHCO<sub>3</sub>, while this was 0.5 M KHCO<sub>3</sub> for the BPM. As explained earlier, in the case of the CEM, additional CO<sub>2</sub> is generated in the solution due to bicarbonate decomposition, which compensates for the salting-out effect of CO<sub>2</sub> at moderate KHCO<sub>3</sub> concentrations. However, the salting-out effect is dominant at very high KHCO<sub>3</sub> concentrations, which affects the CRR. At low electrolyte concentrations, the conductivity is lower, which increases the overpotential and mainly affects the current density.

The variability in the data of the BPM and the CEM is mainly caused by the condition of the membranes and the electrodes. After several experiments, scaling and/or fouling was observed for both membrane types. Therefore, the membranes were replaced after 15 experiments (i.e., after three runs at five pressures). However, a new membrane (i.e., the first run) always gave higher FE, CD, and formate concentration compared to the second and third runs. Furthermore, using a concentrated H<sub>2</sub>SO<sub>4</sub> solution as the anolyte resulted in a yellow sulfur-like deposition on the Ir-MMO anode, which reduces the reactive surface area for the oxygen evolution reaction. This sulfur-like deposition was removed by reaction with a concentrated KOH solution. Similarly, a black deposit was observed on the Sn cathode, which was removed by reaction with a HNO<sub>3</sub> solution. Consistently applying these precautions results in a reproducibility of the experiments to within 5%. Due to the inherent variability in electrochemical experimental data, it is crucial to run multiple repeated experiments. The used tin electrodes were analyzed with a scanning electron microscope (SEM); see the Supporting Information for more details. The observed deposit on the electrode is very likely a tin oxide layer with some metal (e.g., copper) contamination. Agarwal et al.<sup>38</sup> observed similar deposits on Sn electrodes, which were characterized as graphitic type of carbon.

**Effect of Catholyte Flow Rate.** It is well-known that stirring in batch reactors and flow characteristics in continuous flow reactors have a large impact on CO<sub>2</sub> electrolysis.<sup>83–85</sup> Therefore, the effect of catholyte flow rate on CO<sub>2</sub> electrolysis to formate at a cell potential of 3 V using a BPM was investigated. Two flow rates (10 and 20 mL/min) at several CO<sub>2</sub> pressures were tested using 1 M KOH as the anolyte and 0.5 M KHCO<sub>3</sub> as the catholyte. At low pressures, the experiments with a flow rate of 20 mL/min, compared to 10 mL/min, seem to perform slightly better in terms of FE and CD; see Figure 9. This is conforming to expectation, since increasing the flow rate decreases the thickness of the diffusion boundary layer, which improves the mass transport of CO<sub>2</sub> to the electrodes. Often, mass transport is correlated with the Sherwood number,  $Sh = a Sc^b Re^c$ , which is a function of the Schmidt ( $Sc$ ) number and the Reynolds ( $Re$ ) number. In laminar flows between two parallel plates, the exponents  $b$  and  $c$  are 1/3; thus the diffusion boundary layer thickness is proportional to  $\nu^{-1/3}$ , where  $\nu$  is the velocity of the fluid.<sup>70,86</sup> Therefore, it is surprising to see that, at high pressures, the experiments with a flow rate of 10 mL/min have higher FE and CD, which is opposed to the trend observed for low pressures. A possible explanation for this behavior is that mass transfer of CO<sub>2</sub> to the electrode is not the limiting factor at high pressures, since the solubility of CO<sub>2</sub> is relatively high, but other factors (such as proton transport from the BPM to the electrode or increased impurity deposition on the cathode) come into play for increasing flow rates. This explanation is merely a hypothesis, which should be verified in the future with more detailed flow experiments and numerical modeling. Nevertheless, we note that Proietto et al.,<sup>76</sup> Alvarez-Guerra et al.,<sup>87</sup> and Li and Oloman<sup>78,79,88</sup> also observed that increasing the catholyte flow rate does not necessarily improve the performance of electrolytic CO<sub>2</sub> reduction.

**Effect of Cell Potential.** The cell potential can have a significant influence on the selectivity of products in an electrochemical cell. For this reason, CO<sub>2</sub> electrolysis was performed at three different cell potentials (i.e., 3, 3.5, and 4



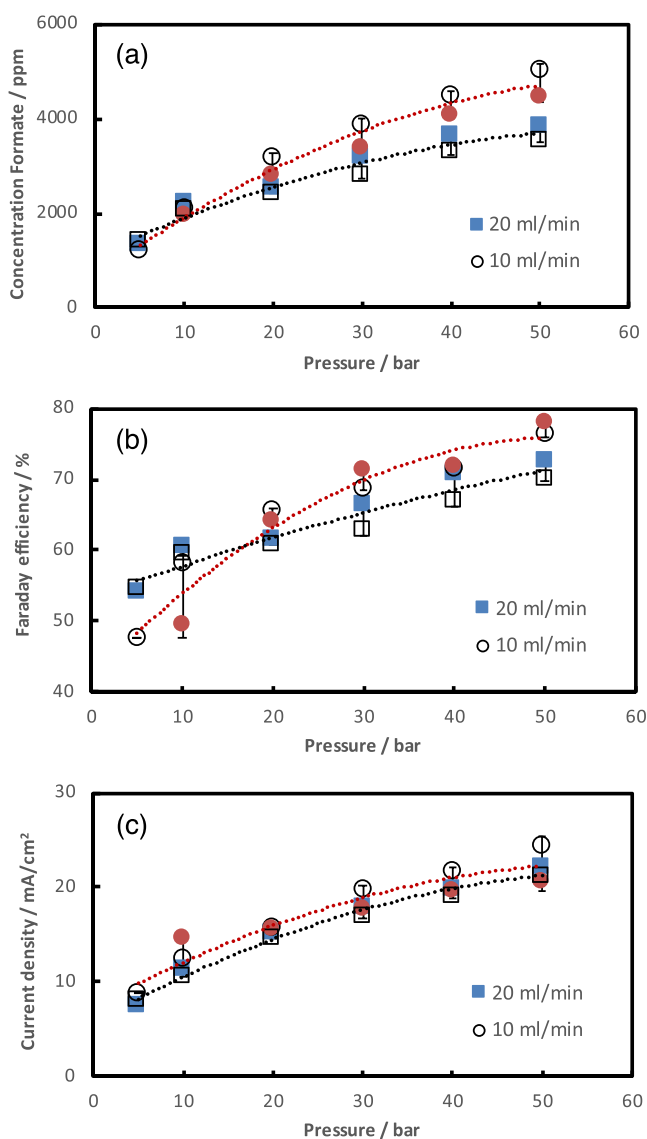


**Figure 9.** Effect of flow rate on the (a) formate production, (b) Faraday efficiency, and (c) current density as a function of pressure for CO<sub>2</sub> electrolysis at 3 V using a BPM. The anolyte, catholyte, and electrolysis time were 1 M KOH, 0.5 M KHCO<sub>3</sub>, and 20 min. Data are shown for two different runs, where the dotted lines represent the arithmetic mean of the results.

V) using a BPM, 1 M KOH as anolyte, 0.5 M KHCO<sub>3</sub> as catholyte, 10 mL/min flow rate, 20 min electrolysis time, and pressures between 10 and 50 bar. The results for the three different cell potentials are depicted in Figure 10. For all three potentials, the concentration of formate, the FE, and the CD increase as the CO<sub>2</sub> pressure is increased. The FE seems to have a maximum around 40 bar for the 3 and 3.5 V experiments, while this is absent at 4 V. However, the FE at 4 V (relative to 3 and 3.5 V) is significantly lower in the low pressure range, which is due to an increased hydrogen production. At low pressures and low current densities, the system is initially located in region 2 of Figure 6. Since the CO<sub>2</sub> solubility and the CD increase at higher pressures, the system shifts first toward region 5, and then (close) to region 1 of Figure 6. An FE of ~90% is attainable at a cell potential of 3.5 V and a current density of ~30 mA/cm<sup>2</sup>, which results in a formate concentration of ~1 wt %. At a cell potential of 4 V

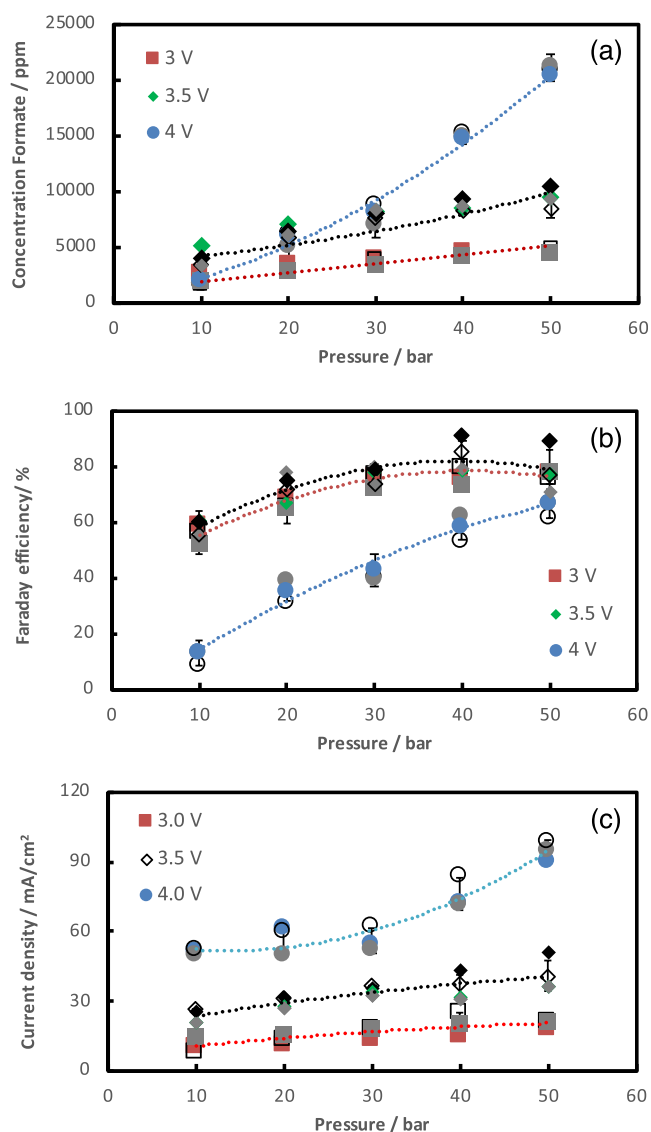
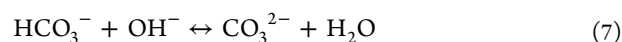


**Figure 10.** Effect of cell potential on the (a) formate production, (b) Faraday efficiency, and (c) current density as a function of pressure for CO<sub>2</sub> electrolysis at 3 (squares), 3.5 (diamonds), and 4 V (circles) using a BPM. The anolyte, catholyte, flow rate, and electrolysis time were 1 M KOH, 0.5 M KHCO<sub>3</sub>, 10 mL/min, and 20 min. Data are shown for three different runs, where the dotted lines represent the arithmetic mean of the results.

and low CO<sub>2</sub> pressures, the system is located in region 7 of Figure 6, and shifts very slowly toward region 1 for higher pressures. An FE of ~65% is attainable at a cell potential of 4 V and a current density of ~100 mA/cm<sup>2</sup>, which results in a formate concentration of ~2 wt %. At high current densities, the CO<sub>2</sub> is quickly consumed and mass transfer starts to limit the process, even at a pressure of 50 bar. Note that increasing the pressure further will have a minor effect, since the solubility of CO<sub>2</sub> in aqueous electrolyte solutions at temperatures below the critical point of CO<sub>2</sub> (~304 K) does not increase significantly at pressures close to or higher than the vapor pressure of CO<sub>2</sub>. At these conditions, the CO<sub>2</sub>-aqueous electrolyte system has a liquid-liquid behavior, which leads to low CO<sub>2</sub> solubilities. Increasing the temperature will improve the mass transfer of CO<sub>2</sub> and the electrode kinetics such that high current densities can be achieved at lower cell potentials,

but the CO<sub>2</sub> solubility in aqueous solvents decreases significantly at higher temperatures. Alternatives to increase the CO<sub>2</sub> solubility are the use of nonaqueous solvents, and electrolytes which exhibit a salting-in effect for CO<sub>2</sub>. An ideal solvent should have a high CO<sub>2</sub> capacity, which is nearly independent of the temperature. In summary, at the given experimental conditions it is extremely challenging to obtain a high FE and a high CD at the same time. In practice, this would mean that one has to compromise between CAPEX, which is dictated by the current density, and OPEX, which is a function of the FE efficiency.

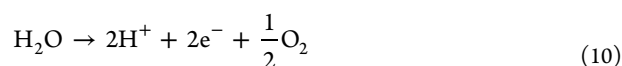
**Combination of Electrodes, Electrolytes, and Membranes.** For a synergistic design of an electrochemical cell it is important that electrodes, electrolytes, and membranes are combined carefully. For example, an efficient operation of the BPM in the reverse bias mode requires an alkaline anolyte to decrease the overpotential for the oxygen evolution reaction (OER). However, it is not practical to use bicarbonate solutions as the anolyte, since the bicarbonate ions will react with the hydroxide ions from the BPM to form carbonates:



The CRR is more efficient in neutral to (slightly) alkaline solutions, but one should not use hydroxides (e.g., KOH) or carbonates (e.g., K<sub>2</sub>CO<sub>3</sub>) as the catholyte, because it will be converted to bicarbonates as the solution is saturated with CO<sub>2</sub>:



Furthermore, using an alkaline solution as a catholyte (e.g., KHCO<sub>3</sub>) in combination with a BPM will result in an additional voltage drop due to reactions of protons with bicarbonate ions at the catholyte–CEL interface. As can be seen in Figure 11, using an acidic anolyte (0.1 M H<sub>2</sub>SO<sub>4</sub>) in combination with a BPM has a dramatic effect on the performance of the electrochemical cell and the CRR. The current density and the amount of formate is reduced drastically compared to the data for an alkaline anolyte (i.e., 1 M KOH). It is not efficient to use acidic anolytes in combination with BPMs, because the overpotential for the OER is higher in acidic media, and an additional potential drop is caused by acid–base reactions at the anolyte–AEL interface. In acidic media, water is split at the anode according to the reaction



The protons will react with the hydroxide ions from the BPM at the anolyte–AEL interface to cause an unnecessary potential drop, which can be estimated using a Nernst-like equation:

$$V_{\text{loss}} \sim \frac{2.303RT}{nF} \log\left(\frac{[\text{H}^+]^{\text{anolyte}}}{[\text{H}^+]^{\text{AEL}}}\right) \approx 0.059\Delta\text{pH} \quad (11)$$

where  $R$ ,  $T$ ,  $n$ ,  $F$ ,  $[\text{H}^+]^i$ , and  $\Delta\text{pH}$  are the ideal gas constant, (room) temperature, charge of a proton, Faraday's constant, concentration of protons in the anolyte and AEL, and the pH difference between the anolyte and the AEL, respectively. Assuming that the concentration of hydroxide ions in the AEL is 1 M (i.e., the pH is 14) and the pH of 0.1 M H<sub>2</sub>SO<sub>4</sub> is

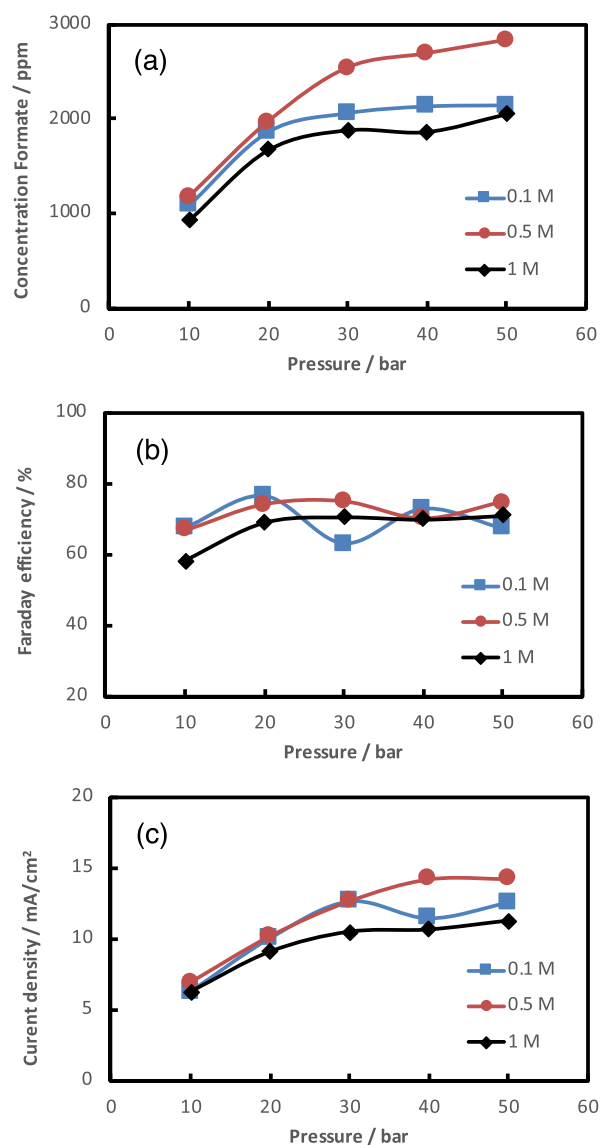


**Figure 11.** Effect of acidic anolyte on the (a) formate production, (b) Faraday efficiency, and (c) current density as a function of pressure for CO<sub>2</sub> electrolysis at 3.5 V using a BPM. The anolyte, flow rate, and electrolysis time were 0.1 M H<sub>2</sub>SO<sub>4</sub>, 10 mL/min, and 20 min. Three different concentrations of KHCO<sub>3</sub> was used as the catholyte: 0.1 (squares), 0.5 (circles), and 1 M (diamonds).

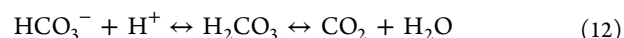
around 1, the potential drop is approximately 0.77 V. In contrast to BPMs, CEMs require acidic anolytes to function properly. Therefore, one should carefully select anolytes and catholytes for CO<sub>2</sub> electrolysis using BPMs/CEMs. In addition, it is important to select electrode materials/catalysts that have a high activity toward the desired oxidation/reduction reactions, and a high stability in acidic and alkaline environments. Recently, McCrory et al.<sup>89</sup> screened a large number of electrocatalysts for the HER/OER in acidic and alkaline solutions. Similar protocols should be used to screen electrocatalysts for the CRR in acidic, neutral, and alkaline environments.

**Comparison between BPMs and CEMs for CO<sub>2</sub> Electrolysis.** The use of BPMs and CEMs for CO<sub>2</sub> electrolysis has a couple of advantages and disadvantages; see Table 1.<sup>49,51,90–97</sup> The main advantage of a BPM is that it can maintain a constant pH gradient over time when no acids or

**Table 1. Advantages and Disadvantages of Bipolar Membranes (BPMs) and Cation Exchange Membranes (CEMs) for CO<sub>2</sub> Electrolysis**<sup>49,51,90–97</sup>

| membrane      | BPM                                 | CEM                              |
|---------------|-------------------------------------|----------------------------------|
| advantages    | + maintains constant pH             | + low price                      |
|               | + low product crossover             | + low potential drop             |
|               | + low electrolyte contamination     | + easy manufacturing             |
|               | + acidification and basification    | + high stability/lifetime        |
| disadvantages | – high price                        | – high product crossover         |
|               | – complex manufacturing             | – high electrolyte contamination |
|               | – short lifetime                    | – acidic anolyte                 |
|               | – low stability in strong bases     | – pH imbalance                   |
|               | – delamination of layers            |                                  |
|               | – limits on high ion concentrations |                                  |

bases are formed as products.<sup>53,70,71</sup> This is not the case for CEMs, which continuously change the pH balance of both compartments as cations are transported through the membrane. The consequence of this is that the anolyte is contaminated with cations from the catholyte and vice versa, which in the longer term will require purification of the electrolytes. Other advantages of BPMs include low product crossover/losses, the possibility to acidify and basify without the addition of acids and bases, and less fouling when the membrane is operated in the reverse-bias mode.<sup>48,49,51</sup> The disadvantage of BPMs include (1) a high price, which is a consequence of using complex manufacturing procedures to laminate the layers; (2) a low stability of the anion exchange layer, especially in strong alkaline solutions; (3) a limit on electrolyte/product concentration to prevent crossover and deterioration of water splitting efficiency due to transport limitations; and (4) a short lifetime due to delamination of the layers.<sup>49,51,94</sup> The latter is mainly caused by an abrupt startup/shutdown leading to accumulation of water on the interface and due to bicarbonate crossover, which is converted in the interfacial region of the BPM to CO<sub>2</sub> according to the reaction



The CO<sub>2</sub> expands at the membrane interface as soon the reactor is depressurized, which leads to blistering and delamination of the layers.

The advantages of CEMs are (1) a low price, which is related to the easy manufacturing procedure; (2) a low potential drop, due to the lower thickness of the membrane; and (3) high stability of the cation exchange layer, which increases the lifetime.<sup>49,51,94</sup> However, the disadvantages of CEMs are more severe compared to BPMs: (1) a high product crossover/loss; (2) the acidic environment, which inhibits the OER and requires noble metals; and (3) contamination of the anolyte with cations from the catholyte and vice versa, which will require expensive electrolyte purification steps downstream of the process. Due to the crossover of ions and products, the pH of the anolyte and catholyte changes continuously, which can adversely affect the performance of CO<sub>2</sub> electrolysis. Note that the crossover of formate can be inhibited to some extent by selecting a proper CEM.

**Current Status of CO<sub>2</sub> Electroreduction to Formic Acid/Formate.** In Table 2, a summary of recent studies on CO<sub>2</sub> electrolysis to formic acid/formate in continuous flow electrolyzers using Sn-based GDEs and plates is provided. Clearly, GDE-based CO<sub>2</sub> electroreduction yields higher CD, FA concentration, and FA production rate. However, it is important to note the CD and FA production rate in all the studies were calculated based on the geometric surface area, which can be significantly different from the real electrochemical surface area.<sup>98,99</sup> The relatively high FA concentration reported by Del Castillo et al.<sup>100</sup> and Yang et al.<sup>101</sup> for the GDE-based processes is mainly a consequence of using small amounts (around 0.2 mL) of catholyte and low flow rate/surface area ratios. The concentration of formic acid decreased significantly as the flow rate was increased. Nevertheless, the single pass FA concentration of Yang et al. is to the best of our knowledge the highest reported so far in the literature. The key of the three-compartment process of Dioxide Materials studied by Yang et al.<sup>101</sup> and Kaczur et al.<sup>102</sup> is an imidazolium-based anion exchange membrane (Sustainion), which exhibits a high conductivity and stability for CO<sub>2</sub>

**Table 2. Comparison of CO<sub>2</sub> Electrolysis to Formic Acid/Formate in Continuous Flow Electrolyzers Using Sn-Based Gas Diffusion Electrodes and Plates**

| condition  | ref 100     | ref 101                 | ref 87      | ref 76  | this work              |
|--|-------------|-------------------------|-------------|---|------------------------|
| mode of operation                                    | single pass | single pass             | single pass | recycled  | recycled               |
| temperature (K)                                      | ambient     | ambient                 | ambient     | ambient   | ambient                |
| pressure (bar)                                       | 1           | 1                       | 1           | 30  | 50                     |
| cathode  | Sn/C-GDE    | Sn/C-GDE                | Sn plate    | Sn plate  | Sn plate               |
| anode  | Ir-MMO      | IrO <sub>2</sub>        | Ir-MMO      | Ti/IrO <sub>2</sub> -Ta <sub>2</sub> O <sub>5</sub> | Ir-MMO                 |
| cation exchange membrane                             | Nafion 117  | Nafion 324 <sup>a</sup> | Nafion 117  | no membrane   | Fumasep BPM            |
| anion exchange membrane                              | –           | Sustainion <sup>a</sup> | –           | no membrane   | Fumasep BPM            |
| geometric surface area of cathode (cm <sup>2</sup> ) | 10.0        | 5                       | 10          | 9   | 80                     |
| flow rate/area of cathode (mL/min·cm <sup>2</sup> )  | 0.07        | 0.02                    | 2.3         | 3.3   | 0.125                  |
| cell voltage (V)                                     | 4.3         | 3.3                     | 2.79        | 6.5 <sup>b</sup>                                    | 3.5 (4.0) <sup>c</sup> |
| current density (mA/cm <sup>2</sup> )                | 200         | 140                     | 12.25       | 50  | 30 (100)               |
| concentration of formic acid (wt %)                  | 1.68        | 9.4                     | 0.005       | 1.26  | 1.0 (2.0)              |
| Faraday efficiency of formic acid (%)                | 42.3        | 94                      | 71.4        | 82.5  | 90 (65)                |
| formic acid production rate (mmol/m <sup>2</sup> ·s) | 4.38        | 6.8                     | 0.46        | 2.1   | 2 (4)                  |
| max operation time (h)                               | 1.5         | 142                     | 1.5         | 60  | 0.33                   |

<sup>a</sup>A three-compartment cell with two different types of membranes was used. <sup>b</sup>Cell potential data obtained from Proietto et al.<sup>76</sup> through personal communication. <sup>c</sup>Data in parentheses are for a cell potential of 4.0 V.

electrolysis. Yang et al. also showed the importance of selecting CEMs to prevent formate crossover. Alvarez-Guerra et al.<sup>87</sup> used a low pressure continuous flow electrolyzer to convert CO<sub>2</sub> to formic acid/formate. These authors obtained a relatively high FE, but the concentration of FA was very low. Proietto et al.<sup>76,103</sup> used a high pressure (up to 30 bar) undivided filter-press cell with a Sn plate as cathode to convert CO<sub>2</sub> to formic acid. The data reported by Proietto et al. shows that the performance of the cell was stable up to 20 h, but deteriorated rapidly afterward. The results reported in this work are (slightly) better than those of Proietto et al., although we have used a cathode with a larger surface area.

For a commercially viable process it is important that all the components of the cell (e.g., membranes, anodes, and cathodes) are stable for a sufficiently long term. To the best of our knowledge, only the Sustainion-based CO<sub>2</sub> electro-reduction process of Dioxide Materials has demonstrated stable operation for more than 500 h for formic acid and up to 4000 h for CO without showing significant loss of activity.<sup>101,102</sup> In this work, we have focused on the reproducibility of the results and long-term stability tests will be performed in a follow-up study.

## CONCLUSIONS

The electrochemical reduction of CO<sub>2</sub> to value-added products will play an important role in power-to-X (P2X) concepts where renewable energy sources, instead of hydrocarbons, are used to produce chemicals and fuels. Before CO<sub>2</sub> utilization by the electrochemical route can be applied at a practical scale, a number of challenges need to be overcome. These include the poor stability and selectivity of the catalyst, the low solubility of CO<sub>2</sub>, the separation of dilute products from electrolyte solutions, and the large overpotentials required to perform the reactions that increase the power input/cost of the products. Here, we have used a high pressure semicontinuous batch electrolyzer to efficiently convert CO<sub>2</sub> to formic acid/formate. The effects of CO<sub>2</sub> pressure, cell potential, electrolyte concentration, flow rate, and two types of membranes—a bipolar membrane (BPM) and a cation exchange membrane (CEM)—on the current density (CD) and Faraday efficiency (FE) for formate were investigated. The FE and the CD increase sharply with increasing CO<sub>2</sub> pressure. The results show that an FE of ~90% is attainable at a pressure of 40–50 bar, a cell potential of 3.5 V and a CD of ~30 mA/cm<sup>2</sup>. Up to 2 wt % formate was produced at a cell potential of 4 V and a CD of ~100 mA/cm<sup>2</sup>, but at a significantly lower FE of 65%. The results also indicate that a moderate flow rate and catholyte (KHCO<sub>3</sub>) concentration should be used to maximize the FE and CD. Although the operating principles of a BPM and a CEM are fundamentally different, they showed similar performances for CO<sub>2</sub> electrolysis in terms of the FE and the CD. Nevertheless, BPMs and CEMs have some inherent advantages and disadvantages, which have been discussed in detail. In contrast to CEMs, BPMs can maintain a constant pH gradient over the membrane and have a low liquid product crossover, which is crucial for the economics of a large-scale CO<sub>2</sub> electrolysis process. We have demonstrated that increasing the pressure has a beneficial effect on the performance of electrolytic CO<sub>2</sub> reduction to formic acid/formate.

## ASSOCIATED CONTENT

### Supporting Information

The Supporting Information is available free of charge on the ACS Publications website at DOI: 10.1021/acs.iecr.8b04944.

Plot of pH as a function of CO<sub>2</sub> pressure in aqueous sodium bicarbonate solutions; SEM images and EDX spectra of the used tin electrodes (PDF)

## AUTHOR INFORMATION

### Corresponding Author

\*E-mail: t.j.h.vlugt@tudelft.nl.

### ORCID

Mahinder Ramdin: 0000-0002-8476-7035

J. P. Martin Trusler: 0000-0002-6403-2488

Thijs J. H. Vlugt: 0000-0003-3059-8712

### Notes

The authors declare no competing financial interest.

## ACKNOWLEDGMENTS

The authors thank Michel van den Brink for his help with the ion chromatograph. The project (TEEI116076: Direct electrochemical conversion of CO<sub>2</sub> to formic acid (P2FA)) is being carried out with a subsidy from the Dutch Ministry of Economic Affairs, under the scheme Joint Industry Projects, executed by RVO (Rijksdienst voor Ondernemend Nederland). T.J.H.V. acknowledges NWO—CW (Chemical Sciences) for a VICI grant.

## REFERENCES

- (1) Gattrell, M.; Gupta, N.; Co, A. Electrochemical Reduction of CO<sub>2</sub> to Hydrocarbons to Store Renewable Electrical Energy and Upgrade Biogas. *Energy Convers. Manage.* **2007**, *48*, 1255–1265.
- (2) Seh, Z. W.; Kibsgaard, J.; Dickens, C. F.; Chorkendorff, I.; Nørskov, J. K.; Jaramillo, T. F. Combining Theory and Experiment in Electrocatalysis: Insights into Materials Design. *Science* **2017**, *355*, No. eaad4998.
- (3) Foit, S. R.; Vinke, I. C.; de Haart, L. G. J.; Eichel, R.-A. Power-to-Syngas: An Enabling Technology for the Transition of the Energy System? *Angew. Chem., Int. Ed.* **2017**, *56*, 5402–5411.
- (4) Institute for Sustainable Process Technology. *Power to Ammonia*; Institute for Sustainable Process Technology: 2017; p 51.
- (5) Schemme, S.; Samsun, R. C.; Peters, R.; Stolten, D. Power-to-fuel as a Key to Sustainable Transport Systems - An Analysis of Diesel Fuels Produced from CO<sub>2</sub> and Renewable Electricity. *Fuel* **2017**, *205*, 198–221.
- (6) Sternberg, A.; Bardow, A. Power-to-What? - Environmental Assessment of Energy Storage Systems. *Energy Environ. Sci.* **2015**, *8*, 389–400.
- (7) Karlsson, K. B.; Petrovic, S.; Abad Hernando, D. Global outlook on energy technology development. In *Accelerating the Clean Energy Revolution - Perspectives on Innovation Challenges: DTU International Energy Report 2018*; Technical University of Denmark (DTU): 2018.
- (8) Azuma, M.; Watanabe, M. Electrodes in Low-Temperature Aqueous KHCO<sub>3</sub> Media. *J. Electrochem. Soc.* **1990**, *137*, 1772–1778.
- (9) Bushuyev, O. S.; De Luna, P.; Dinh, C. T.; Tao, L.; Saur, G.; van de Lagemaat, J.; Kelley, S. O.; Sargent, E. H. What Should We Make with CO<sub>2</sub> and How Can We Make It? *Joule* **2018**, *2*, 825–832.
- (10) Gattrell, M.; Gupta, N.; Co, A. A Review of the Aqueous Electrochemical Reduction of CO<sub>2</sub> to Hydrocarbons at Copper. *J. Electroanal. Chem.* **2006**, *594*, 1–19.
- (11) Kuhl, K. P.; Cave, E. R.; Abram, D. N.; Jaramillo, T. F. New Insights into the Electrochemical Reduction of Carbon Dioxide on Metallic Copper Surfaces. *Energy Environ. Sci.* **2012**, *5*, 7050.

- (12) Sheng, W.; Kattel, S.; Yao, S.; Yan, B.; Liang, Z.; Hawxhurst, C. J.; Wu, Q.; Chen, J. G. Electrochemical Reduction of CO<sub>2</sub> to Synthesis Gas with Controlled CO/H<sub>2</sub> Ratios. *Energy Environ. Sci.* **2017**, *10*, 1180–1185.
- (13) Dinh, C.-T.; Burdyny, T.; Kibria, M. G.; Seifitokaldani, A.; Gabardo, C. M.; Garcia de Arquer, F. P.; Kiani, A.; Edwards, J. P.; De Luna, P.; Bushuyev, O. S.; Zou, C.; Quintero-Bermudez, R.; Pang, Y.; Sinton, D.; Sargent, E. H. CO<sub>2</sub> Electroreduction to Ethylene via Hydroxide-mediated Copper Catalysis at an Abrupt Interface. *Science* **2018**, *360*, 783–787.
- (14) Hori, Y. In *Solar to Chemical Energy Conversion*; Sugiyama, M., Fujii, K., Nakamura, S., Eds.; Lecture Notes in Energy 32; Springer International Publishing: Cham, Switzerland, 2016; pp 191–211. DOI: 10.1007/978-3-319-25400-5\_12.
- (15) Whipple, D. T.; Kenis, P. J. A. Prospects of CO<sub>2</sub> Utilization via Direct Heterogeneous Electrochemical Reduction. *J. Phys. Chem. Lett.* **2010**, *1*, 3451–3458.
- (16) Lu, X.; Leung, D. Y. C.; Wang, H.; Leung, M. K. H.; Xuan, J. Electrochemical Reduction of Carbon Dioxide to Formic Acid. *ChemElectroChem* **2014**, *1*, 836–849.
- (17) Kortlever, R.; Shen, J.; Schouten, K. J. P.; Calle-Vallejo, F.; Koper, M. T. M. Catalysts and Reaction Pathways for the Electrochemical Reduction of Carbon Dioxide. *J. Phys. Chem. Lett.* **2015**, *6*, 4073–4082.
- (18) Feaster, J. T.; Shi, C.; Cave, E. R.; Hatsukade, T.; Abram, D. N.; Kuhl, K. P.; Hahn, C.; Nørskov, J. K.; Jaramillo, T. F. Understanding Selectivity for the Electrochemical Reduction of Carbon Dioxide to Formic Acid and Carbon Monoxide on Metal Electrodes. *ACS Catal.* **2017**, *7*, 4822–4827.
- (19) Chaplin, R. P.; Wragg, A. A. Effects of Process Conditions and Electrode Material on Reaction Pathways for Carbon Dioxide Electroreduction with Particular Reference to Formate Formation. *J. Appl. Electrochem.* **2003**, *33*, 1107–1123.
- (20) Jhong, H.-R. M.; Ma, S.; Kenis, P. J. Electrochemical Conversion of CO<sub>2</sub> to Useful Chemicals: Current Status, Remaining Challenges, and Future Opportunities. *Curr. Opin. Chem. Eng.* **2013**, *2*, 191–199.
- (21) Zheng, X.; et al. Sulfur-Modulated Tin Sites Enable Highly Selective Electrochemical Reduction of CO<sub>2</sub> to Formate. *Joule* **2017**, *1*, 794–805.
- (22) Irabien, A.; Alvarez-Guerra, M.; Albo, J.; Dominguez-Ramos, A. In *Electrochemical Water and Wastewater Treatment*; Elsevier, 2018; pp 29–59. DOI: 10.1016/B978-0-12-813160-2.00002-X.
- (23) Liu, X.; Xiao, J.; Peng, H.; Hong, X.; Chan, K.; Nørskov, J. K. Understanding Trends in Electrochemical Carbon Dioxide Reduction Rates. *Nat. Commun.* **2017**, *8*, 15438.
- (24) Ooka, H.; Figueiredo, M. C.; Koper, M. T. M. Competition between Hydrogen Evolution and Carbon Dioxide Reduction on Copper Electrodes in Mildly Acidic Media. *Langmuir* **2017**, *33*, 9307–9313.
- (25) Zhang, Y.-J.; Sethuraman, V.; Michalsky, R.; Peterson, A. A. Competition between CO<sub>2</sub> Reduction and H<sub>2</sub> Evolution on Transition-Metal Electrocatalysts. *ACS Catal.* **2014**, *4*, 3742–3748.
- (26) Hara, K. Electrochemical Reduction of CO<sub>2</sub> on a Cu Electrode under High Pressure. *J. Electrochem. Soc.* **1994**, *141*, 2097.
- (27) Hara, K.; Kudo, A.; Sakata, T. Electrochemical Reduction of Carbon Dioxide Under High Pressure on Various Electrodes in an Aqueous Electrolyte. *J. Electroanal. Chem.* **1995**, *391*, 141–147.
- (28) Hara, K.; Sakata, T. Large Current Density CO<sub>2</sub> Reduction under High Pressure Using Gas Diffusion Electrodes. *Bull. Chem. Soc. Jpn.* **1997**, *70*, 571–576.
- (29) Kaneco, S.; Iiba, K.; Katsumata, H.; Suzuki, T.; Ohta, K. Electrochemical Reduction of High Pressure CO<sub>2</sub> at a Cu Electrode in Cold Methanol. *Electrochim. Acta* **2006**, *51*, 4880–4885.
- (30) Todoroki, M.; Hara, K.; Kudo, A.; Sakata, T. Electrochemical Reduction of High Pressure CO<sub>2</sub> at Pb, Hg and In Electrodes in an Aqueous KHCO<sub>3</sub> Solution. *J. Electroanal. Chem.* **1995**, *394*, 199–203.
- (31) Mahmood, M. N.; Masheder, D.; Harty, C. J. Use of Gas-diffusion Electrodes for High-rate Electrochemical Reduction of Carbon Dioxide. I. Reduction at Lead, Indium- and Tin-impregnated Electrodes. *J. Appl. Electrochem.* **1987**, *17*, 1159–1170.
- (32) Kai, T.; Zhou, M.; Duan, Z.; Henkelman, G. A.; Bard, A. J. Detection of CO<sub>2</sub><sup>\*</sup> in the Electrochemical Reduction of Carbon Dioxide in N, N -Dimethylformamide by Scanning Electrochemical Microscopy. *J. Am. Chem. Soc.* **2017**, *139*, 18552–18557.
- (33) Costentin, C.; Robert, M.; Savéant, J.-M. Catalysis of the Electrochemical Reduction of Carbon Dioxide. *Chem. Soc. Rev.* **2013**, *42*, 2423–2436.
- (34) Bidault, F.; Brett, D.; Middleton, P.; Brandon, N. Review of Gas Diffusion Cathodes for Alkaline Fuel Cells. *J. Power Sources* **2009**, *187*, 39–48.
- (35) Cindrella, L.; Kannan, A.; Lin, J.; Saminathan, K.; Ho, Y.; Lin, C.; Wertz, J. Gas Diffusion Layer for Proton Exchange Membrane Fuel Cells - A Review. *J. Power Sources* **2009**, *194*, 146–160.
- (36) Park, S.; Lee, J.-W.; Popov, B. N. A Review of Gas Diffusion Layer in PEM Fuel Cells: Materials and Designs. *Int. J. Hydrogen Energy* **2012**, *37*, 5850–5865.
- (37) Weng, L.-C.; Bell, A. T.; Weber, A. Z. Modeling Gas-diffusion Electrodes for CO<sub>2</sub> Reduction. *Phys. Chem. Chem. Phys.* **2018**, *20*, 16973–16984.
- (38) Agarwal, A. S.; Zhai, Y.; Hill, D.; Sridhar, N. The Electrochemical Reduction of Carbon Dioxide to Formate/Formic Acid: Engineering and Economic Feasibility. *ChemSusChem* **2011**, *4*, 1301–1310.
- (39) Jouny, M.; Luc, W.; Jiao, F. General Techno-Economic Analysis of CO<sub>2</sub> Electrolysis Systems. *Ind. Eng. Chem. Res.* **2018**, *57*, 2165–2177.
- (40) Pérez-Fortes, M.; Schöneberger, J. C.; Boulamanti, A.; Harrison, G.; Tzimas, E. Formic Acid Synthesis Using CO<sub>2</sub> as Raw Material: Techno-economic and Environmental Evaluation and Market Potential. *Int. J. Hydrogen Energy* **2016**, *41*, 16444–16462.
- (41) Spurgeon, J. M.; Kumar, B. A Comparative Technoeconomic Analysis of Pathways for Commercial Electrochemical CO<sub>2</sub> Reduction to Liquid Products. *Energy Environ. Sci.* **2018**, *11*, 1536–1551.
- (42) Verma, S.; Kim, B.; Jhong, H.-R. M.; Ma, S.; Kenis, P. J. A. A Gross-Margin Model for Defining Technoeconomic Benchmarks in the Electroreduction of CO<sub>2</sub>. *ChemSusChem* **2016**, *9*, 1972–1979.
- (43) Moret, S.; Dyson, P. J.; Laurenczy, G. Direct Synthesis of Formic Acid from Carbon Dioxide by Hydrogenation in Acidic Media. *Nat. Commun.* **2014**, *5*, 4017.
- (44) Rahbari, A.; Ramdin, M.; van den Broeke, L. J. P.; Flugt, T. J. H. Combined Steam Reforming of Methane and Formic Acid To Produce Syngas with an Adjustable H<sub>2</sub>:CO Ratio. *Ind. Eng. Chem. Res.* **2018**, *57*, 10663–10674.
- (45) Leitner, W. Carbon Dioxide as a Raw Material: The Synthesis of Formic Acid and Its Derivatives from CO<sub>2</sub>. *Angew. Chem., Int. Ed. Engl.* **1995**, *34*, 2207–2221.
- (46) Rumayor, M.; Dominguez-Ramos, A.; Irabien, A. Formic Acid Manufacture: Carbon Dioxide Utilization Alternatives. *Appl. Sci.* **2018**, *8*, 914.
- (47) Hietala, J.; Vuori, A.; Johnsson, P.; Pollari, I.; Reutemann, W.; Kieczka, H. *Ullmann's Encyclopedia of Industrial Chemistry*; Wiley-VCH Verlag GmbH & Co. KGaA: Weinheim, Germany, 2016; pp 1–22.
- (48) Li, Y. C.; Yan, Z.; Hitt, J.; Wycisk, R.; Pintauro, P. N.; Mallouk, T. E. Bipolar Membranes Inhibit Product Crossover in CO<sub>2</sub> Electrolysis Cells. *Adv. Sustain. Syst.* **2018**, *2*, 1700187.
- (49) Strathmann, H.; Grabowski, A.; Eigenberger, G. Ion-Exchange Membranes in the Chemical Process Industry. *Ind. Eng. Chem. Res.* **2013**, *52*, 10364–10379.
- (50) Strathmann, H.; Krol, J. J.; Rapp, H.-J.; Eigenberger, G. Limiting Current Density and Water Dissociation in Bipolar Membranes. *J. Membr. Sci.* **1997**, *125*, 123–142.
- (51) Tongwen, X. Electrodialysis Processes with Bipolar Membranes (EDBM) in Environmental Protection-A Review. *Resour. Conserv. Recycl.* **2002**, *37*, 1–22.
- (52) Vargas-Barbosa, N. M.; Geise, G. M.; Hickner, M. A.; Mallouk, T. E. Assessing the Utility of Bipolar Membranes for use in

Photoelectrochemical Water-Splitting Cells. *ChemSusChem* **2014**, *7*, 3017–3020.

(53) Vermaas, D. A.; Sassenburg, M.; Smith, W. A. Photo-assisted Water Splitting with Bipolar Membrane Induced pH Gradients for Practical Solar Fuel Devices. *J. Mater. Chem. A* **2015**, *3*, 19556–19562.

(54) Mafé, S.; Ramírez, P. Electrochemical Characterization of Polymer Ion-exchange Bipolar Membranes. *Acta Polym.* **1997**, *48*, 234–250.

(55) Mafé, S.; Manzanares, J. A.; Ramirez, P. Model for Ion Transport in Bipolar Membranes. *Phys. Rev. A: At., Mol., Opt. Phys.* **1990**, *42*, 6245–6248.

(56) Ramírez, P.; Aguilera, V.; Manzanares, J.; Mafé, S. Effects of Temperature and Ion Transport on Water Splitting in Bipolar Membranes. *J. Membr. Sci.* **1992**, *73*, 191–201.

(57) Simons, R. Preparation of a High Performance Bipolar Membrane. *J. Membr. Sci.* **1993**, *78*, 13–23.

(58) Simons, R.; Khanarian, G. Water Dissociation in Bipolar Membranes: Experiments and Theory. *J. Membr. Biol.* **1978**, *38*, 11–30.

(59) Simons, R. A. Mechanism for Water Flow in Bipolar Membranes. *J. Membr. Sci.* **1993**, *82*, 65–73.

(60) Simons, R. A. Novel Method for Preparing Bipolar Membranes. *Electrochim. Acta* **1986**, *31*, 1175–1177.

(61) Huang, C.; Xu, T. Electrodialysis with Bipolar Membranes for Sustainable Development. *Environ. Sci. Technol.* **2006**, *40*, 5233–5243.

(62) Eisaman, M. D.; Alvarado, L.; Larner, D.; Wang, P.; Littau, K. A. CO<sub>2</sub> Desorption Using High-Pressure Bipolar Membrane Electrodialysis. *Energy Environ. Sci.* **2011**, *4*, 4031.

(63) Eisaman, M. D.; Alvarado, L.; Larner, D.; Wang, P.; Garg, B.; Littau, K. A. CO<sub>2</sub> Separation Using Bipolar Membrane Electrodialysis. *Energy Environ. Sci.* **2011**, *4*, 1319–1328.

(64) Grew, K. N.; McClure, J. P.; Chu, D.; Kohl, P. A.; Ahlfield, J. M. Understanding Transport at the Acid-Alkaline Interface of Bipolar Membranes. *J. Electrochem. Soc.* **2016**, *163*, F1572–F1587.

(65) Li, Y. C.; Zhou, D.; Yan, Z.; Gonçalves, R. H.; Salvatore, D. A.; Berlinguette, C. P.; Mallouk, T. E. Electrolysis of CO<sub>2</sub> to Syngas in Bipolar Membrane-Based Electrochemical Cells. *ACS Energy Lett.* **2016**, *1*, 1149–1153.

(66) McDonald, M. B.; Ardo, S.; Lewis, N. S.; Freund, M. S. Use of Bipolar Membranes for Maintaining Steady-State pH Gradients in Membrane-Supported, Solar-Driven Water Splitting. *ChemSusChem* **2014**, *7*, 3021–3027.

(67) Luo, J.; Vermaas, D. A.; Bi, D.; Hagfeldt, A.; Smith, W. A.; Grätzel, M. Bipolar Membrane-Assisted Solar Water Splitting in Optimal pH. *Adv. Energy Mater.* **2016**, *6*, 1600100.

(68) Reiter, R. S.; White, W.; Ardo, S. Communication-Electrochemical Characterization of Commercial Bipolar Membranes under Electrolyte Conditions Relevant to Solar Fuels Technologies. *J. Electrochem. Soc.* **2016**, *163*, H3132–H3134.

(69) Salvatore, D. A.; Weekes, D. M.; He, J.; Dettelbach, K. E.; Li, Y. C.; Mallouk, T. E.; Berlinguette, C. P. Electrolysis of Gaseous CO<sub>2</sub> to CO in a Flow Cell with a Bipolar Membrane. *ACS Energy Lett.* **2018**, *3*, 149–154.

(70) Vermaas, D. A.; Wiegman, S.; Nagaki, T.; Smith, W. A. Ion Transport Mechanisms in Bipolar Membranes for (Photo)-electrochemical Water Splitting. *Sustain. Energy Fuels* **2018**, *2*, 2006–2015.

(71) Vermaas, D. A.; Smith, W. A. Synergistic Electrochemical CO<sub>2</sub> Reduction and Water Oxidation with a Bipolar Membrane. *ACS Energy Lett.* **2016**, *1*, 1143–1148.

(72) Zhou, X.; Liu, R.; Sun, K.; Chen, Y.; Verlage, E.; Francis, S. A.; Lewis, N. S.; Xiang, C. Solar-Driven Reduction of 1 atm of CO<sub>2</sub> to Formate at 10% Energy-Conversion Efficiency by Use of a TiO<sub>2</sub>-Protected III-V Tandem Photoanode in Conjunction with a Bipolar Membrane and a Pd/C Cathode. *ACS Energy Lett.* **2016**, *1*, 764–770.

(73) Mani, K. Electrodialysis Water Splitting Technology. *J. Membr. Sci.* **1991**, *58*, 117–138.

(74) Jaime-Ferrer, J. S.; Couallier, E.; Viers, P.; Durand, G.; Rakib, M. Three-Compartment Bipolar Membrane Electrodialysis for Splitting of Sodium Formate into Formic Acid and Sodium Hydroxide: Role of Diffusion of Molecular Acid. *J. Membr. Sci.* **2008**, *325*, 528–536.

(75) Jaime-Ferrer, J.; Couallier, E.; Viers, P.; Rakib, M. Two-Compartment Bipolar Membrane Electrodialysis for Splitting of Sodium Formate into Formic Acid and Sodium Hydroxide: Modelling. *J. Membr. Sci.* **2009**, *328*, 75–80.

(76) Proietto, F.; Schiavo, B.; Galia, A.; Scialdone, O. Electrochemical Conversion of CO<sub>2</sub> to HCOOH at Tin Cathode in a Pressurized Undivided Filter-Press Cell. *Electrochim. Acta* **2018**, *277*, 30–40.

(77) Ku, H. Notes on the Use of Propagation of Error Formulas. *J. Res. Natl. Bur. Stand., Sect. C* **1966**, *70C*, 263.

(78) Li, H.; Oloman, C. Development of a Continuous Reactor for the Electro-Reduction of Carbon Dioxide to Formate - Part 1: Process Variables. *J. Appl. Electrochem.* **2006**, *36*, 1105–1115.

(79) Li, H.; Oloman, C. Development of a Continuous Reactor for the Electro-Reduction of Carbon Dioxide to Formate - Part 2: Scale-up. *J. Appl. Electrochem.* **2007**, *37*, 1107–1117.

(80) Zhong, H.; Fujii, K.; Nakano, Y. Effect of KHCO<sub>3</sub> Concentration on Electrochemical Reduction of CO<sub>2</sub> on Copper Electrode. *J. Electrochem. Soc.* **2017**, *164*, F923–F927.

(81) Chen, L. D.; Urushihara, M.; Chan, K.; Nørskov, J. K. Electric Field Effects in Electrochemical CO<sub>2</sub> Reduction. *ACS Catal.* **2016**, *6*, 7133–7139.

(82) Singh, M. R.; Goodpaster, J. D.; Weber, A. Z.; Head-Gordon, M.; Bell, A. T. Mechanistic Insights into Electrochemical Reduction of CO<sub>2</sub> over Ag Using Density Functional Theory and Transport Models. *Proc. Natl. Acad. Sci. U. S. A.* **2017**, *114*, E8812–E8821.

(83) Weekes, D. M.; Salvatore, D. A.; Reyes, A.; Huang, A.; Berlinguette, C. P. Electrolytic CO<sub>2</sub> Reduction in a Flow Cell. *Acc. Chem. Res.* **2018**, *51*, 910–918.

(84) Endrodi, B.; Bencsik, G.; Darvas, F.; Jones, R.; Rajeshwar, K.; Janáky, C. Continuous-Flow Electroreduction of Carbon Dioxide. *Prog. Energy Combust. Sci.* **2017**, *62*, 133–154.

(85) Scialdone, O.; Galia, A.; Nero, G. L.; Proietto, F.; Sabatino, S.; Schiavo, B. Electrochemical Reduction of Carbon Dioxide to Formic Acid at a Tin Cathode in Divided and Undivided Cells: Effect of Carbon Dioxide Pressure and Other Operating Parameters. *Electrochim. Acta* **2016**, *199*, 332–341.

(86) Sonin, A. A.; Isaacson, M. S. Optimization of Flow Design in Forced Flow Electrochemical Systems, with Special Application to Electrodialysis. *Ind. Eng. Chem. Process Des. Dev.* **1974**, *13*, 241–248.

(87) Alvarez-Guerra, M.; Del Castillo, A.; Irabien, A. Continuous Electrochemical Reduction of Carbon Dioxide into Formate Using a Tin Cathode: Comparison with Lead Cathode. *Chem. Eng. Res. Des.* **2014**, *92*, 692–701.

(88) Li, H.; Oloman, C. The Electro-Reduction of Carbon Dioxide in a Continuous Reactor. *J. Appl. Electrochem.* **2005**, *35*, 955–965.

(89) McCrory, C. C. L.; Jung, S.; Ferrer, I. M.; Chatman, S. M.; Peters, J. C.; Jaramillo, T. F. Benchmarking Hydrogen Evolving Reaction and Oxygen Evolving Reaction Electrocatalysts for Solar Water Splitting Devices. *J. Am. Chem. Soc.* **2015**, *137*, 4347–4357.

(90) Alabi, A.; AlHajaj, A.; Cseri, L.; Szekeley, G.; Budd, P.; Zou, L. Review of Nanomaterials-Assisted Ion Exchange Membranes for Electromembrane Desalination. *npj Clean Water* **2018**, *1*, 10.

(91) Dekel, D. R. Review of Cell Performance in Anion Exchange Membrane Fuel Cells. *J. Power Sources* **2018**, *375*, 158–169.

(92) Hagesteijn, K. F. L.; Jiang, S.; Ladewig, B. P. A Review of the Synthesis and Characterization of Anion Exchange Membranes. *J. Mater. Sci.* **2018**, *53*, 11131–11150.

(93) Jaroszek, H.; Dydo, P. Ion-Exchange Membranes in Chemical Synthesis - A Review. *Open Chem.* **2016**, *14*, 1–19.

(94) Luo, T.; Abdu, S.; Wessling, M. Selectivity of Ion Exchange Membranes: A Review. *J. Membr. Sci.* **2018**, *555*, 429–454.

- (95) Maurya, S.; Shin, S.-H.; Kim, Y.; Moon, S.-H. A Review on Recent Developments of Anion Exchange Membranes for Fuel Cells and Redox Flow Batteries. *RSC Adv.* **2015**, *5*, 37206–37230.
- (96) Park, C. H.; Lee, S. Y.; Hwang, D. S.; Shin, D. W.; Cho, D. H.; Lee, K. H.; Kim, T.-W.; Kim, T.-W.; Lee, M.; Kim, D.-S.; Doherty, C. M.; Thornton, A. W.; Hill, A. J.; Guiver, M. D.; Lee, Y. M. Nanocrack-Regulated Self-Humidifying Membranes. *Nature* **2016**, *532*, 480–483.
- (97) Yee, R.; Rozendal, R.; Zhang, K.; Ladewig, B. Cost Effective Cation Exchange Membranes: A Review. *Chem. Eng. Res. Des.* **2012**, *90*, 950–959.
- (98) Trasatti, S.; Petrii, O. Real Surface Area Measurements in Electrochemistry. *J. Electroanal. Chem.* **1992**, *327*, 353–376.
- (99) Łukaszewski, M. Electrochemical Methods of Real Surface Area Determination of Noble Metal Electrodes - an Overview. *Int. J. Electrochem. Sci.* **2016**, *11*, 4442–4469.
- (100) Del Castillo, A.; Alvarez-Guerra, M.; Solla-Gullón, J.; Sáez, A.; Montiel, V.; Irabien, A. Sn Nanoparticles on Gas Diffusion Electrodes: Synthesis, Characterization and Use for Continuous CO<sub>2</sub> Electroreduction to Formate. *J. CO<sub>2</sub> Util.* **2017**, *18*, 222–228.
- (101) Yang, H.; Kaczur, J. J.; Sajjad, S. D.; Masel, R. I. Electrochemical Conversion of CO<sub>2</sub> to Formic Acid Utilizing Sustainion Membranes. *J. CO<sub>2</sub> Util.* **2017**, *20*, 208–217.
- (102) Kaczur, J. J.; Yang, H.; Liu, Z.; Sajjad, S. D.; Masel, R. I. Carbon Dioxide and Water Electrolysis Using New Alkaline Stable Anion Membranes. *Front. Chem.* **2018**, *6*, 1–16.
- (103) Proietto, F.; Galia, A.; Scialdone, O. Electrochemical Conversion of CO<sub>2</sub> to HCOOH at Tin Cathode: Development of a Theoretical Model and Comparison with Experimental Results. *ChemElectroChem* **2019**, *6*, 162–172.